FISEVIER

Contents lists available at ScienceDirect

### Thin Solid Films

journal homepage: www.elsevier.com/locate/tsf



# Improved resistive switching properties by nitrogen doping in tungsten oxide thin films



Seok Man Hong <sup>a</sup>, Hee-Dong Kim <sup>a,b</sup>, Min Ju Yun <sup>a</sup>, Ju Hyun Park <sup>a</sup>, Dong Su Jeon <sup>a</sup>, Tae Geun Kim <sup>a,\*</sup>

- <sup>a</sup> School of Electrical Engineering, Korea University, Seoul 136-701, Republic of Korea
- <sup>b</sup> Department of Electrical Engineering, Sejong University, Seoul 134-747, Republic of Korea

#### ARTICLE INFO

Article history: Received 27 January 2014 Received in revised form 9 March 2015 Accepted 20 March 2015 Available online 27 March 2015

Keywords: Resistive switching Resistive random access memories Tungsten oxide Nitrogen doping

#### ABSTRACT

In this study, nitrogen-doped  $WO_x$  thin films are investigated for the improvement of resistive switching (RS) properties. Compared to  $WO_x$  thin films, nitrogen-doped  $WO_x$  thin films exhibit a higher on/off current ratio (a separation of ~2 orders of magnitude), better endurance (>100 cycles), narrower current dispersion, and longer retention characteristics (>10<sup>4</sup> s). Electrical measurements, X-ray diffraction, and X-ray photoelectron spectroscopy demonstrate that nitrogen in  $WO_x$ :N thin films forms WN nanoclusters and  $W_x$  (O, N) phases, which are beneficial to improve the RS properties in  $WO_x$  thin films; WN nanoclusters can locally enhance the electric field to form stable conductive filament while  $W_x$  (O, N) phases can suppress random migrations of oxygen ions ( $O^{2-}$ ), leading to stable RS characteristics. Our findings suggest that nitrogen doping method can lead further optimization of the RS characteristics in  $WO_x$  thin films.

© 2015 Elsevier B.V. All rights reserved.

#### 1. Introduction

Resistive random access memory (RRAM) has attracted considerable attention as a candidate for next-generation nonvolatile memory (NVM) because of its non-volatility, high-speed operation, simple structure, and suitability in three-dimensional memory applications [1,2]. At present, many resistive switching (RS) materials have been discovered, such as transition-metal oxides (TMOs) and transition-metal nitrides [3, 4]. Among these materials, TMOs such as NiO, TiO<sub>2</sub>, and WO<sub>x</sub> are promising candidates for use in NVM applications because of their excellent RS characteristics, flexible stoichiometry, and compatibility with complementary metal-oxide-semiconductor processes [5]. However, the unknown physical origins of the RS phenomena must be determined if high-performance RRAM is to be developed.

Among  $TMO_s$ ,  $WO_x$  is very interesting because it can be fabricated using a simple oxygen annealing method with a tungsten plug in back-end-of-line process. According to previous reports on  $WO_x$ -based RRAM, localized conductive filament (CF) formation and rupture are the responsible RS mechanisms [6–8]. However, conventional  $WO_x$  memory cells still have several issues such as high operating currents, a small on/off current ratio, and broad ranges of on/off current levels because of randomly generated localized CFs. Thus, the control of the localized CFs in  $WO_x$  thin films is a key factor when enhancing the RS properties of  $WO_x$ -based RRAM. Several studies have been performed to control CF generation by the insertion of metal doping, and Si introduction [9,10]. Recently, Liu et al. reported that an additional layer of NbO<sub>x</sub>

between the  $WO_{3-x}$  layer and the Pt bottom layer improved the RS properties of a  $WO_x$  memory cell because the  $NbO_x$  layer helps to localize the position of the CF path. Syu et al. reported that the tungsten CF path is limited by the presence of silicon oxide in Si-doped  $WO_x$  thin films.

In this work, we report a nitrogen-doped  $WO_x$ -based RRAM device fabricated using the reactive sputtering method. Nitrogen doping is performed to stabilize the RS properties originating from the randomly generated CFs in  $WO_x$ -based RRAM. A larger on/off ratio (a separation of ~2 orders of magnitude) and a longer retention time (over  $10^4$  s) are achieved by nitrogen doping, compared to an undoped  $WO_x$  memory cell. Therefore, the improvement of RS characteristics in  $WO_x$  thin films with nitrogen doping was investigated.

#### 2. Experimental details

To prepare the samples, Pt bottom electrodes (BEs) with thicknesses of 300 nm were deposited on Ti/SiO $_2$ /Si substrates using a radiofrequency (RF) sputtering system. Undoped and nitrogen-doped 50 nm WO $_x$  thin films were deposited on the BE using reactive sputtering from a tungsten (W) target at room temperature. The base pressure and working pressure for all samples were  $2.67 \times 10^{-4}$  Pa and 1.33 Pa, respectively. For the deposition of the undoped WO $_x$  thin films, the argon and oxygen flow rates were 20 and 10 sccm, respectively. The nitrogen-doped WO $_x$  (WO $_x$ :N) thin film was fabricated by adding nitrogen gas at a flow rate of 5 sccm to the argon–oxygen mixture during undoped WO $_x$  thin film deposition. Next, all samples were annealed in an N $_2$  gas atmosphere at 600 °C for 30 s using rapid thermal annealing. Next, the Ti top electrode (TE) with a thickness of 100 nm and a diameter of 100  $\mu$ m was deposited using a shadow mask to create the metal/insulator/metal RRAM structure.

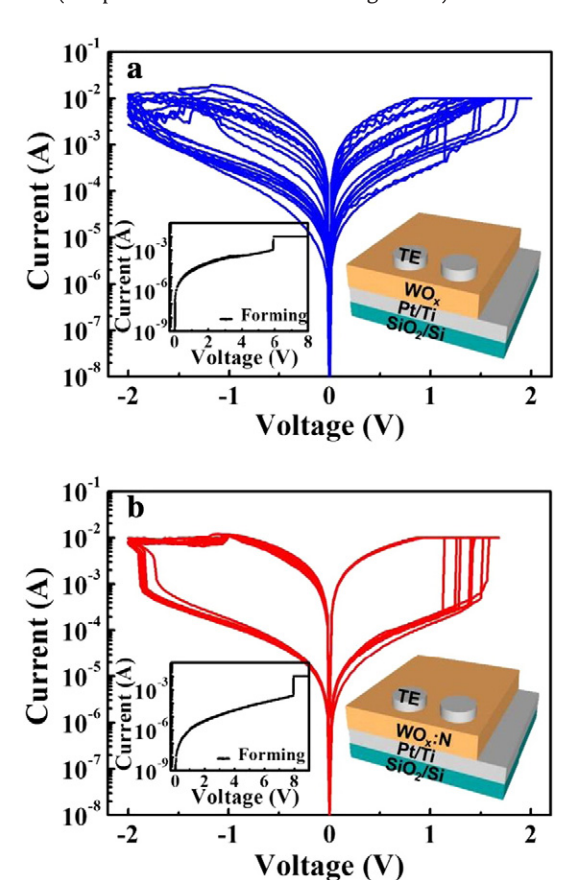
<sup>\*</sup> Corresponding author at: Korea University, Anamdong Seongbukku, Seoul 136-713. E-mail address: tgkim1@korea.ac.kr (T.G. Kim).

The electrical characteristics of the memory devices were measured using a Keithley 4200-SCS semiconductor parameter analyzer. During the tests, the TEs of the samples were connected to a current–voltage (*I–V*) tester, and the BEs were grounded.

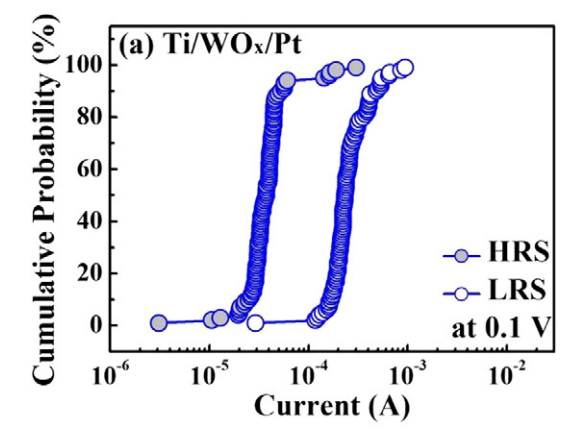
#### 3. Results and discussion

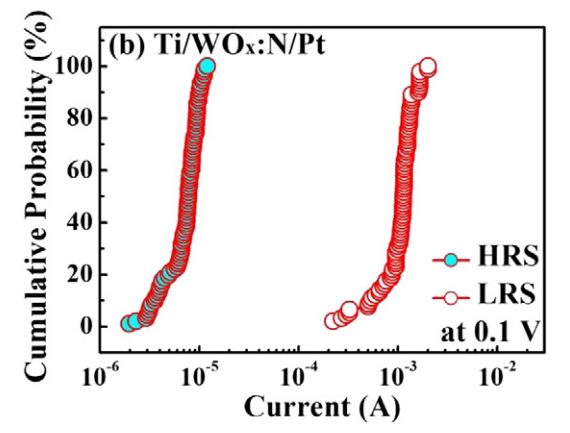
Fig. 1(a) and (b) shows the RS characteristics of the Ti/WO<sub>x</sub>/Pt and Ti/WO<sub>x</sub>:N/Pt cells, respectively. The data are acquired for 100 cycles of switching. All samples experience an irreversible forming process with a compliance current of 10 mA to activate their RS properties, as shown in the inset of Fig. 1(a) and (b). After the forming process, the memory cells are able to switch from the low resistance state (LRS) to the high resistance state (HRS), and counter-clockwise RS is achieved. Both Ti/WO<sub>x</sub>/Pt and Ti/WO<sub>x</sub>:N/Pt devices are switched to the LRS from the HRS in the voltage range between +1 V and +2 V (called the set process) and switched to the HRS from the LRS near the -2 V region (called the reset process). Fig. 1(a) shows the I–V characteristics of the Ti/WO<sub>x</sub>/Pt device measured over a DC sweep; the device displays typical bipolar RS behavior. However, this device exhibits inferior RS characteristics such as a small on/off current ratio and unstable HRS and LRS. The LRS and HRS current levels are different for each DC voltage sweep, which results in unstable LRS and HRS. In contrast, the Ti/WO<sub>x</sub>:N/Pt device exhibits superior RS characteristics, as shown in Fig. 1(b). Compared to the Ti/WO<sub>x</sub>/Pt memory cell, the RS characteristics of the Ti/WO<sub>x</sub>:N/Pt device are significantly improved, namely, the device has more stable LRS and HRS and a large on/off current ratio.

Fig. 2(a) and (b) shows current cumulative probability over 100 DC sweep cycles for the  $Ti/WO_x/Pt$  and  $Ti/WO_x:N/Pt$  memory cells, respectively. It is obvious that the memory window of the  $Ti/WO_x/Pt$  device is very small (a separation of ~0.5 order of magnitude) and that there are



**Fig. 1.** Bipolar I-V characteristics for the (a)  $Ti/WO_x/Pt$  and (b)  $Ti/WO_x$ : N/Pt devices. The data are acquired from the switching of 100 cycles. The insets in (a) and (b) show the irreversible forming process.





**Fig. 2.** Cumulative probability of both the HRS and LRS current levels for the (a)  $Ti/WO_x/Pt$  and (b)  $Ti/WO_x:N/Pt$  devices, respectively.

some data points overlapping between the HRS and LRS, as shown in Fig. 2(a). However, Fig. 2(b) shows a large on/off current ratio (a separation of ~2 orders of magnitude) for the Ti/WO<sub>x</sub>:N/Pt device. These results indicate that nitrogen significantly enhances the RS properties of WO<sub>x</sub> thin films.

To further confirm the performance of the Ti/WO $_x$ /Pt and Ti/WO $_x$ :N/Pt devices, retention characteristics were measured over  $10^4$  s after 100 DC cycles at room temperature. Fig. 3(a) shows the retention characteristics of the Ti/WO $_x$ /Pt device. Similar to the unstable RS behavior of the Ti/WO $_x$ /Pt device in Fig. 1(a), the HRS is unstable, and its current grows continuously with time. For the Ti/WO $_x$ :N/Pt device, however, the LRS and HRS are stable for more than 104 s and have approximately two orders of magnitude of current difference, as shown in Fig. 3(b). These results reveal the excellent nonvolatile properties of the proposed Ti/WO $_x$ :N/Pt memory cell.

The conduction mechanisms of the HRS and LRS were investigated to more clearly understand the RS characteristics. Fig. 4 shows the conduction mechanism of the Ti/WO<sub>x</sub>/Pt and Ti/WO<sub>x</sub>:N/Pt cells. In the HRS region, the *I–V* curves of both samples exhibit ohmic behavior in the low voltage region, but Poole–Frenkel (P–F) emission dominates the current conduction at higher electric fields. The P–F equation can be expressed as  $\ln(J/E) \propto \left(\sqrt{q^3/\pi\epsilon_r\epsilon_0}/rkT\right) \cdot \left(\sqrt{E}\right)$ , where q is the electric charge,  $\epsilon_r$  is the static dielectric constant,  $\epsilon_0$  is the permittivity of the free space, k is the Boltzmann's constant, and T is the temperature. Here, r is the trap coefficient in the insulator and it is reported in the range of 1 to 2 [11]. For example, in the case of normal P–F effect, r is close to 1, while r can be reached to 2 when the non-negligible trap exists in the insulator, which is called the modified P–E emission [12]. Fig. 4(a) and (c) shows the linear dependence of  $\ln(J/E)$  on E1/2. According to the higher degree of slope in P–F emission fitting, we presume that the higher

## Download English Version:

# https://daneshyari.com/en/article/8034223

Download Persian Version:

https://daneshyari.com/article/8034223

<u>Daneshyari.com</u>